

# Enhanced Zeeman splitting in $\text{Ga}_{0.25}\text{In}_{0.75}\text{As}$ quantum point contacts

T. P. Martin,<sup>\*</sup> A. Szorkovszky, A. P. Micolich, and A. R. Hamilton  
*School of Physics, University of New South Wales, Sydney NSW 2052, Australia*

C. A. Marlow, H. Linke, and R. P. Taylor<sup>†</sup>  
*Department of Physics, University of Oregon, Eugene OR 97403, USA*

L. Samuelson  
*Division of Solid State Physics, Lund University, Box 118, S-221 00 Lund, Sweden*  
 (Dated: November 24, 2018)

The strength of the Zeeman splitting induced by an applied magnetic field is an important factor for the realization of spin-resolved transport in mesoscopic devices. We measure the Zeeman splitting for a quantum point contact etched into a  $\text{Ga}_{0.25}\text{In}_{0.75}\text{As}$  quantum well, with the field oriented parallel to the transport direction. We observe an enhancement of the Landé  $g$ -factor from  $|g^*| = 3.8 \pm 0.2$  for the third subband to  $|g^*| = 5.9 \pm 0.6$  for the first subband, six times larger than in GaAs. We report subband spacings in excess of 10 meV, which facilitates quantum transport at higher temperatures.

PACS numbers: 73.21.Hb, 71.70.Ej, 85.75.-d

The control of a charge carrier's spin is typically achieved using an applied magnetic field, and provides an extra degree of freedom that can be utilized for new device functionalities such as spintronics, quantum information, etc.<sup>1,2,3,4</sup> In semiconductor devices, the field  $B$  breaks the degeneracy of the two spin states via the Zeeman effect, resulting in spin-polarized transport, where a particular spin orientation dominates the electrical conductance of the device.<sup>1,2</sup> The Zeeman spin-splitting is given by  $\Delta E_z = g^* \mu_B B$ , where  $g^*$  is the effective Landé  $g$ -factor and  $\mu_B$  is the Bohr magneton. Since the strength of the spin-splitting is governed by  $g^*$ , narrow band-gap materials with a large  $g$ -factor such as GaInAs or InAs are highly desirable in the quest to develop electronic devices that require only the smallest magnetic fields to achieve spin-functional operations.

The small band-gap in the  $\text{Ga}_x\text{In}_{1-x}\text{As}$  material system makes a large  $g$ -factor possible due to mixing of the conduction band electron states with valence band states. For example, in GaInAs quantum wells,  $g$ -factors ranging from 2.9 to 4.4 have been measured<sup>5,6,7,8</sup> – an order of magnitude larger than in equivalent GaAs quantum wells.<sup>6,9</sup> It is thus interesting to know how the  $g$ -factor in lower-dimensional structures will behave, because the additional confinement alters the coupling between the conduction and valence bands. In GaAs quantum point contacts (QPCs), the confinement of electrons to a quasi-one-dimensional system can lead to an enhancement of  $|g^*|$  by as much as a factor of two over its 2D value, with the enhancement increasing as the 1D confinement is strengthened.<sup>10,11</sup> Unexpectedly, the only measurement to date of the  $g$ -factor in a GaInAs QPC<sup>8</sup> gave  $|g^*| \approx 4$  in the 1D limit, showing no clear enhancement over the value of  $|g^*|$  obtained in the 2D reservoirs adjacent to the QPC.<sup>8</sup>

In this letter, we use parallel field measurements (oriented in the plane of the quantum well along the QPC) to

study how the strength of the 1D confinement affects the spin-splitting in an etched  $\text{Ga}_{0.25}\text{In}_{0.75}\text{As}$  QPC. In contrast to the measurements obtained using perpendicular fields by Schäpers *et al.*,<sup>8</sup> we observe a clear enhancement of the  $g$ -factor in the 1D limit of our device. Our result is consistent with the 1D enhancement observed in GaAs QPCs, which was also measured using parallel field techniques.<sup>10,11</sup> The key difference between our measurements and those of Ref. 8 is the field direction, and we use this to explain why 1D  $g$ -factor enhancement was not observed in their study.

Our QPC is etched into a GaInAs/InP modulation-doped heterostructure, where a 2D electron gas (2DEG) is confined to a 9 nm thick  $\text{Ga}_{0.25}\text{In}_{0.75}\text{As}$  quantum well.<sup>12</sup> The QPC investigated is  $\sim 160$  nm long and  $\sim 120$  nm wide, and fabricated on a Hall bar mesa featuring NiGeAu Ohmic contacts. A Ti/Au top-gate, deposited uniformly over the mesa, is used to tune the Fermi energy  $E_F$  and thus change the number of occupied subbands  $n$  in the QPC. All measurements were performed in a <sup>4</sup>He cryostat with a base temperature of 1.3 K. Standard four-probe and lock-in amplification techniques were used to measure the differential conductance  $G = dI/dV$  through the QPC at a frequency of 17 Hz and constant excitation voltage of 100  $\mu\text{V}$  (300  $\mu\text{V}$  for source-drain biasing). The 2D carrier density and mobility were  $5.6\text{--}6.8 \times 10^{11} \text{ cm}^{-2}$  and  $1.3\text{--}2.2 \times 10^5 \text{ cm}^2/\text{Vs}$  respectively within the range of applied gate voltages presented here ( $-6.0$  to  $1.5$  V). Our 2D density and mobility, gallium fraction  $x = 0.25$ , and quantum well width are very similar to the values reported in Ref. 8.

The blue line in Fig. 1(b) shows the conductance  $G$  of the QPC at  $B = 0$ , demonstrating clear plateaux as a function of gate voltage  $V_g$ . The plateaux are a consequence of the 1D confinement in the QPC, where each occupied subband contributes  $2e^2/h$  to the conductance. An in-plane magnetic field  $B_{\parallel}$  was applied parallel to

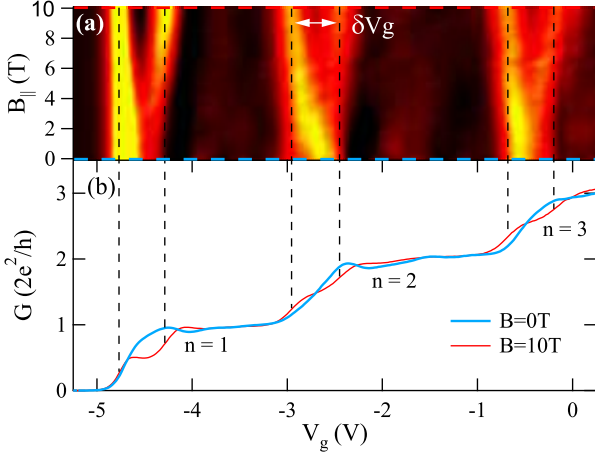


FIG. 1: (Color online) Zeeman splitting for the first three subbands of the QPC. (a) Transconductance  $dG/dV_g$  as a function of gate voltage  $V_g$  (horizontal axis) and magnetic field  $B_{||}$  (vertical axis). Regions of yellow and red correspond to a large amplitude of  $dG/dV_g$ , indicating the locations of subband transitions. (b) Conductance  $G$  vs gate voltage  $V_g$  for  $B_{||} = 0$  T (thick blue line) and 10 T (thin red line). Dashed lines in (a) indicate the region of the plot corresponding to the colored traces in (b).

the direction of transport in the QPC to induce Zeeman splitting. At  $B_{||} = 10$  T, the spin-degeneracy is lifted (red line in Fig. 1(b)) and the conductance is quantized in units  $e^2/h$ . The evolution of the spin splitting with applied magnetic field is shown in Fig. 1(a), where the transconductance  $dG/dV_g$  is plotted as a function of the gate voltage and magnetic field. The light regions mark the 1D subband edges, corresponding to the rises between conductance plateaux where  $dG/dV_g$  is maximum. The spin-splitting  $\Delta E_z$  increases with applied magnetic field, which is observed as an increasingly large splitting  $\delta V_g$  between the bright regions in Fig. 1(a).

Unfortunately, the splitting  $\Delta E_z$  cannot be obtained directly from Fig. 1(a), which only gives  $\delta V_g$ . To calculate the  $g$ -factor, it is necessary to convert  $\delta V_g$  into an energy scale, which is achieved by measuring the splitting in gate voltage due to an applied d.c. source-drain bias  $V_{sd}$ . We do this using the method developed by Patel *et al.*<sup>10</sup> that combines measurements of the splitting due to the field  $\delta V_g/\delta B_{||}$  (Fig. 1(a)) with measurements of the splitting due to the source-drain bias  $\delta V_g/\delta V_{sd}$  to give the absolute value of the  $g$ -factor:

$$|g^*| = \frac{1}{\mu_B} \frac{d(\Delta E_z)}{dB_{||}} = \frac{1}{\mu_B} \frac{d(\Delta E_z)}{dV_g} \frac{dV_g}{dB_{||}} = \frac{e}{\mu_B} \frac{\delta V_{sd}}{\delta V_g} \frac{\delta V_g}{\delta B_{||}} \quad (1)$$

The source-drain bias measurements are shown in Fig. 2, where the transconductance  $dG/dV_g$  is plotted as a function of  $V_g$  and  $V_{sd}$  at  $B_{||} = 0$  (data have been corrected for the d.c. bias dropped across the series resistance). Similar to Fig. 1(a), the light regions correspond to the transitions between 1D subbands (large  $dG/dV_g$ ),

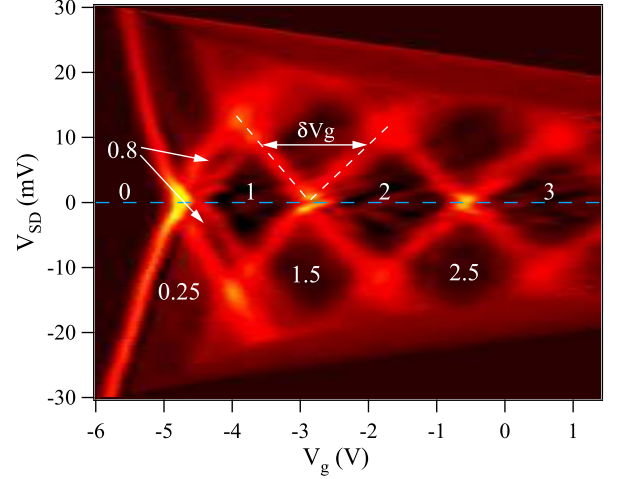


FIG. 2: (Color online) Transconductance  $dG/dV_g$  plotted as a function of gate voltage  $V_g$  (horizontal axis) and source-drain bias  $V_{sd}$  (vertical axis) at  $B_{||} = 0$ . Regions of yellow and red correspond to a large amplitude of  $dG/dV_g$ , indicating the locations of subband transitions. The conductance  $G$  is labeled on each plateau in units of  $2e^2/h$ . Arrows indicate the  $G \approx 0.8(2e^2/h)$  plateaux that are linked to the '0.7 feature'.<sup>13,14</sup> The blue dashed line indicates the region of the plot that is equivalent to the blue trace in Fig. 1(b).

marking the 1D subband edges. As the applied bias  $V_{sd}$  is increased, the subband transitions (light regions) split in gate voltage by  $\delta V_g$ , and conductance plateaux at half-integer  $2e^2/h$  appear between the split transitions.<sup>13,14</sup> Since the splitting  $\delta V_g$  is directly proportional to  $eV_{sd}$ , the energy scales associated with  $\delta V_g$  in Fig. 2 are obtained by calculating  $e\delta V_{sd}/\delta V_g$ .<sup>13,14</sup>

The transconductance maxima in Fig. 2 cross when the applied source-drain bias is equal to the subband spacing:  $\Delta E_{n,n+1} = eV_{sd}$ ,<sup>13,14</sup> allowing the subband spacing to be directly extracted from Fig. 2. Subband spacings calculated from these crossing points are listed in Table I and exceed 10 meV, consistent with the subband spacings obtained from magnetic depopulation measurements in Ref. 12. Additional structure is observed in Fig. 2. In Refs. 13,14 the '0.7 feature' evolves into plateaux with  $G \approx 0.85(2e^2/h)$  at finite source-drain bias. In Fig. 2, we observe similar 'shoulder' plateaux with  $G \approx 0.8(2e^2/h)$ , despite there being no clear '0.7 feature' at  $V_{sd} = 0$ . Oscillatory structure is also observed on the conductance plateaux in Fig. 2, which has recently been linked to standing waves in the QPC<sup>15</sup> and will be discussed elsewhere.

Data extracted from Figs. 1 and 2 are presented in Table I for the first three subbands. A few technical comments need to be made regarding this data. First, because of the '0.7 feature' and its analogs,<sup>14</sup> the spin-splitting in Fig. 1(a) does not converge to zero<sup>10,11</sup> at  $B_{||} = 0$  for the  $n = 1$  and  $n = 2$  subbands. Nevertheless, this does not affect the  $g$ -factor as defined in Eqn. (1) as long as the spin-split subbands can be clearly

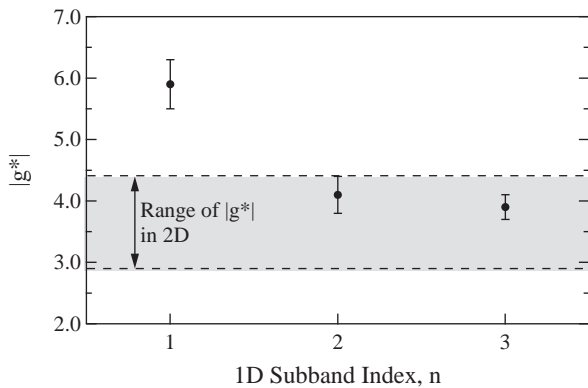


FIG. 3: Landé  $g$ -factor  $|g^*|$  in the QPC as a function of 1D subband index  $n$ . Dashed lines bound the range of  $|g^*|$  previously measured for 2D  $\text{Ga}_x\text{In}_{1-x}\text{As}$  systems.<sup>5,6,7,8</sup>

resolved ( $B_{\parallel} \gtrsim 2$  T).<sup>10,11</sup> Second, the errors calculated for  $\delta V_g/\delta B_{\parallel}$  and  $e\delta V_{sd}/\delta V_g$  reflect the uncertainty in determining the maxima in  $dG/dV_g$ . The values of  $|g^*|$  in Table I are plotted as a function of  $n$  in Fig. 3. For the  $n = 2$  and  $n = 3$  subbands, we find that  $|g^*|$  falls within the range previously reported for 2D  $\text{Ga}_x\text{In}_{1-x}\text{As}$  systems.<sup>5,6,7,8</sup> However, in contrast with Ref. 8, we obtain  $|g^*| = 5.9 \pm 0.6$  for  $n = 1$ , confirming the presence of a 1D enhancement in our  $\text{Ga}_{0.25}\text{In}_{0.75}\text{As}$  QPC.

Previous measurements of the Zeeman splitting in surface-gated GaInAs QPCs were performed with fields  $3 \text{ T} \leq B_{\perp} \leq 8 \text{ T}$  applied perpendicular to the quantum well,<sup>8</sup> which results in magnetic lengths  $9 \text{ nm} \leq l_B \leq 15 \text{ nm}$ . Considering the QPC studied in Ref. 8 had a litho-

graphic width of 160 nm, it is likely that  $l_B$  was less than half the electrostatic width of the QPC for this field range. This places the measurement in the quantum Hall regime, where the electrons are confined to edge states and no longer sense the 1D confinement in the QPC. Thus measurements in the QPC and the adjacent 2D reservoirs will be governed by the same physics, which may explain why the  $g^*$  measured for the QPC was consistent with measurements of  $g^*$  in 2D systems.<sup>5,6,7,8</sup> Furthermore, data were only obtained for the  $n = 1$  subband,<sup>8</sup> so it was not possible to observe a potential enhancement of  $g^*$  as the system became more one-dimensional. In contrast, our data are obtained with an in-plane magnetic field and the quantum Hall effect is absent. Our measurements show the  $g$ -factor of the 1D channel becoming larger as the system becomes more one-dimensional, as has been observed in GaAs.<sup>10,11</sup>

In summary, we have demonstrated that 1D confinement in a narrow-gap semiconductor such as GaInAs can result in a significant enhancement of the Zeeman splitting. Although the enhancement in  $|g^*|$  is consistent with the trend observed in GaAs QPCs,<sup>10,11</sup> the magnitude of  $|g^*|$  measured for GaInAs QPCs is 6 times greater. Additionally, the subband spacing in our devices is quite large.<sup>12</sup> Combined, the large  $g$ -factors and subband spacings found in etched GaInAs QPCs make them suitable for applications requiring spin-sensitivity at higher temperatures and with small magnetic fields.

We acknowledge financial support by the Australian Research Council, the National Science Foundation, and the Research Corporation.

\* Electronic address: tmartin@phys.unsw.edu.au

† Department of Physics and Astronomy, University of Canterbury, Christchurch 8140, New Zealand

<sup>1</sup> S. A. Wolf, D. D. Awschalom, R. A. Buhrman, J. M. Daughton, S. von Molnar, M. L. Roukes, A. Y. Chtchelkanova, and D. M. Treger, *Science* **294**, 1488 (2001).

<sup>2</sup> J. M. Elzerman, R. Hanson, L. H. W. van Beveren, B. Witkamp, L. M. K. Vandersypen, and L. P. Kouwenhoven, *Nature* **430**, 431 (2004).

<sup>3</sup> N. J. Craig, J. M. Taylor, E. A. Lester, C. M. Marcus, M. P. Hanson, and A. C. Gossard, *Science* **304**, 565 (2004).

<sup>4</sup> N. Tombros, S. J. van der Molen, and B. J. van Wees, *Phys. Rev. B* **73**, 233403 (2006).

<sup>5</sup> D. L. Vehse, S. G. Hummel, H. M. Cox, F. DeRosa, and S. J. Allen, *Phys. Rev. B* **33**, 5862 (1986).

<sup>6</sup> M. Dobers, J. P. Vieren, Y. Guldner, P. Bove, F. Omnes, and M. Razeghi, *Phys. Rev. B* **40**, 8075 (1989).

<sup>7</sup> I. G. Savel'ev, A. M. Kreshchuk, S. V. Novikov, A. Y. Shik, G. Remenyi, G. Kovács, B. Pödör, and G. Gombos, *J. Phys.: Condens. Matter* **8**, 9025 (1996).

<sup>8</sup> T. Schäpers, V. A. Guzenko, and H. Hardtdegen, *Appl. Phys. Lett.* **90**, 122107 (2007).

<sup>9</sup> M. Dobers, K. von Klitzing, and G. Weimann, *Phys. Rev. B* **38**, 5453 (1988).

<sup>10</sup> N. K. Patel, J. T. Nicholls, L. Martín-Moreno, M. Pepper, J. E. F. Frost, D. A. Ritchie, and G. A. C. Jones, *Phys. Rev. B* **44**, 10973 (1991).

<sup>11</sup> K. J. Thomas, J. T. Nicholls, M. Y. Simmons, M. Pepper, D. R. Mace, and D. A. Ritchie, *Phys. Rev. Lett.* **77**, 135 (1996).

<sup>12</sup> T. P. Martin, C. A. Marlow, L. Samuelson, A. R. Hamilton, H. Linke, and R. P. Taylor, *Phys. Rev. B* **77**, 103811 (2008).

<sup>13</sup> N. K. Patel, J. T. Nicholls, L. Martín-Moreno, M. Pepper, J. E. F. Frost, D. A. Ritchie, and G. A. C. Jones, *Phys. Rev. B* **44**, 13549 (1991).

<sup>14</sup> A. Kristensen, H. Bruus, A. E. Hansen, J. B. Jensen, P. E. Lindelof, C. J. Marckmann, J. Nygård, C. B. Sørensen, F. Beuscher, A. Forchel, and M. Michel, *Phys. Rev. B* **62**, 10950 (2000).

<sup>15</sup> P. E. Lindelof and M. Aagesen, *J. Phys.: Condens. Matter* **20**, 164207 (2008).

TABLE I: Subband-dependent parameters of the QPC.

Parameter		$n = 1$	$n = 2$	$n = 3$
$\delta V_g / \delta B_{\parallel}$	(V/T)	$0.0295 \pm 0.0015$	$0.0371 \pm 0.0015$	$0.0500 \pm 0.0015$
$e\delta V_{sd} / \delta V_g$	(meV/V)	$11.5 \pm 0.6$	$6.4 \pm 0.3$	$4.4 \pm 0.2$
$ g^* $	- -	$5.9 \pm 0.6$	$4.1 \pm 0.3$	$3.8 \pm 0.2$
$\Delta E_{n,n+1}$	(meV)	$13.1 \pm 0.5$	$11.1 \pm 0.5$	$9.9 \pm 0.5$